Chapter 9: Boundary Layer (Chap. 8 Bernard)

Consider high Re flow (1) around streamlined/slender body for which viscous effects are confined to a narrow boundary layer near the solid surface/wall or (2) for free shear flows, i.e., jets, wakes and mixing layers for which the vorticity is similarly confined to a narrow region. In both cases Prandtl's boundary layer theory is applicable.

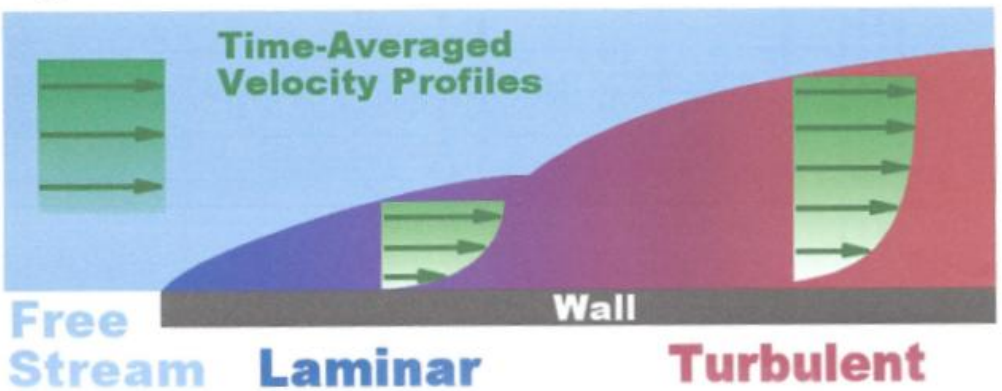

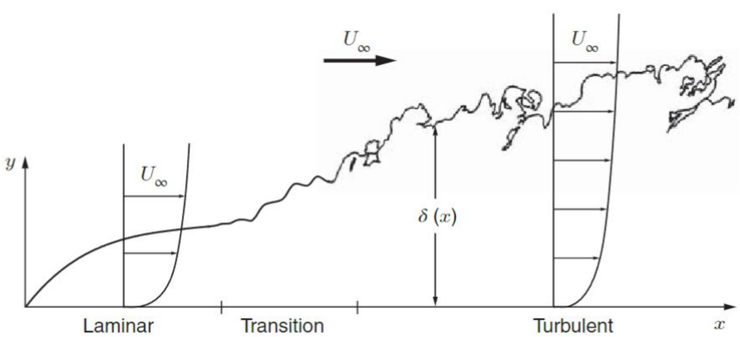

Figure 8.1 Turbulent boundary layer over a flat plate.

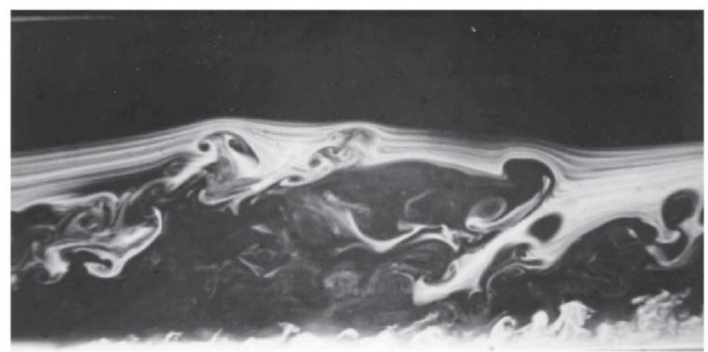

Figure 8.2 Smoke visualization of a turbulent boundary layer at $R_\theta = 3000$ [1].

Inner (viscous) and outer (inviscid; often potential) flow divided by sharp corrugated interface defined by intermittency function.

Stability and transition: arguably top of list of difficult/complex fluid mechanics problems still at forefront of research.

$$Re_{x_{crit}} \sim 4 \times 10^5 \qquad Re_x = \frac{U_\infty x}{\nu}$$

1. Stable laminar flow near the leading edge.
2. Unstable two-dimensional Tollmien–Schlichting waves.
3. Development of three-dimensional unstable waves and hairpin eddies.
4. Vortex breakdown at regions of high localized shear.
5. Cascading vortex breakdown into fully three-dimensional fluctuations.
6. Formation of turbulent spots at locally intense fluctuations.
7. Coalescence of spots into fully turbulent flow.

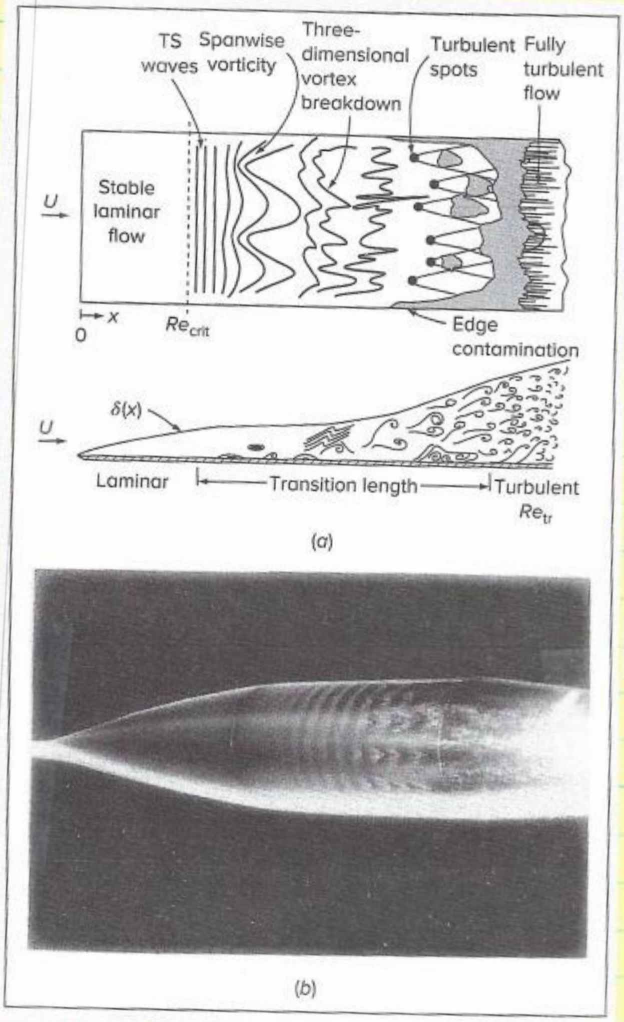

FIGURE 5-28
Description of the boundary-layer transition process: (*a*) idealized sketch of flat-plate flow and (*b*) smoke visualization of flow with transition induced early by acoustic input at Re_L = 814,000 and 500 Hz. [*Courtesy of J.T. Kegelman and T.J Mueller, University of Notre Dame*].

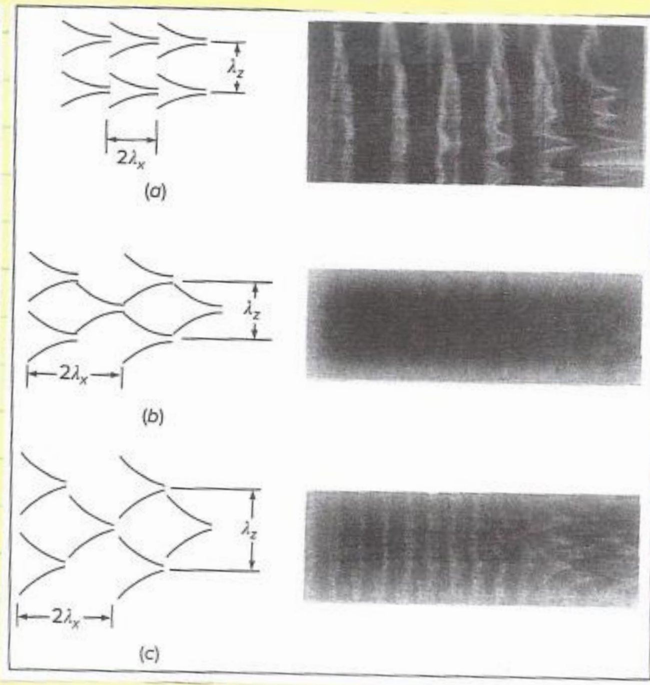

FIGURE 5-26
Patterns of unstable vortex breakdown in a boundary layer: (*a*) K-type ($u'/U_\infty \approx 1$ percent) aligne[illegible] phase and similar to a Tollmien–Schlichting wave; (*b*) C-type (0.3 percent) staggered subharmonic with $\lambda_z \approx 1.5\lambda$ (*c*) H-type (0.6 percent) staggered subharmonic with $\lambda_z \approx 0.7\lambda_x$. [*Courtesy of Dr. William S. Saric*].

8.1 General Properties

Common structure other wall flows (e.g., channel and pipe), except stronger influence of departure from log law in the outer layer. Also $\delta(x)$ not constant as per h and D.

$$\overline{U}(x,\delta) = 0.99U_\infty(x)$$

Where the factor 0.99 is chosen arbitrarily.

δ^*: displacement thickness (δ_1) defined using equivalent discharge:

$$\int_0^\infty \overline{U}(x,y)dy = \int_{\delta_1(x)}^\infty U_\infty(x)dy$$

Or equivalently:

$$\delta_1(x) = \int_0^\infty \left(1 - \frac{\overline{U}(x,y)}{U_\infty(x)}\right)dy$$

Measure of distance outer flow displaced by BL.

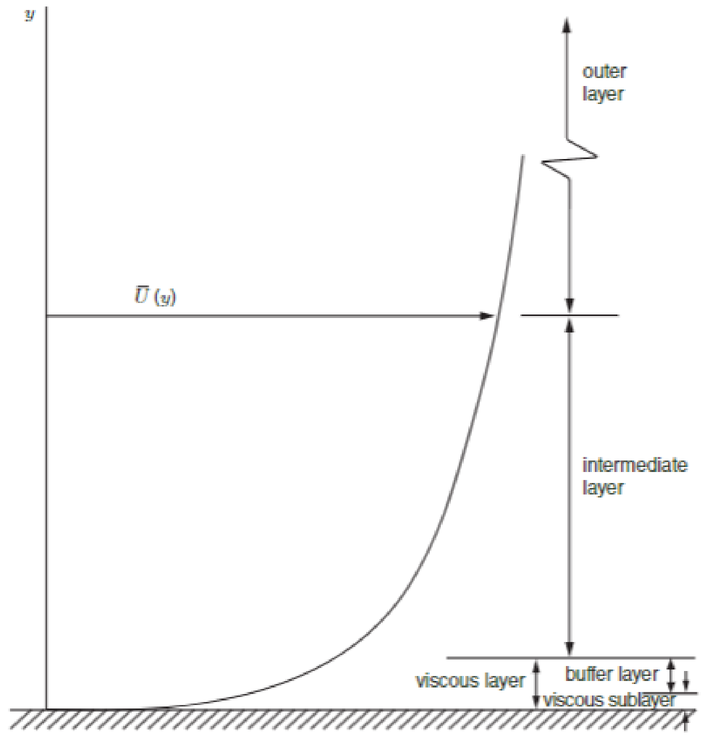

Figure 8.3 Boundary layer zones, not drawn to scale.

Outer Flow

$$\frac{U_\infty^2}{2} + \frac{\overline{p}}{\rho} = \frac{U_0^2}{2} + \frac{p_0}{\rho} = \text{reference values}$$

$$\overline{p_x} = -\rho U_\infty U_{\infty_x}$$

θ: momentum thickness

$$\theta(x) \equiv \int_0^\infty \frac{\overline{U}(x,y)}{U_\infty(x)}\left(1 - \frac{\overline{U}(x,y)}{U_\infty(x)}\right)dy$$

Measure of loss of momentum due to BL.

Different Reynolds numbers can be defined using these quantities:

$$Re_x = \frac{U_\infty x}{\nu} \quad R_\delta = \frac{U_\infty \delta}{\nu} \quad R_{\delta_1} = \frac{U_\infty \delta_1}{\nu} \quad R_\theta = \frac{U_\infty \theta}{\nu}$$

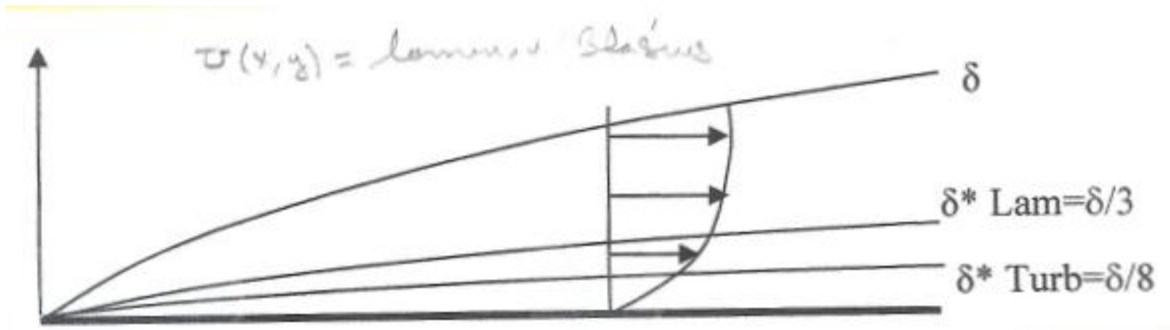

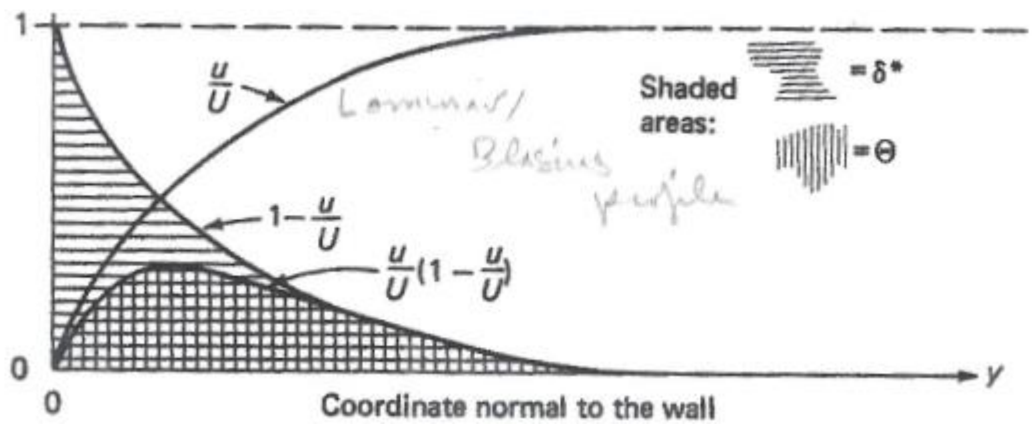

Intermittency

$\delta(x) =$ mean BL thickness → intermittent.

$\gamma =$ fraction of time flow at y/δ is completely turbulent.

Early formulation for $\frac{\partial \overline{p}}{\partial x} = 0$:

$$\gamma(y) = \frac{1}{2}\left(1 - \operatorname{erf}\left(5\left(\frac{y}{\delta} - 0.78\right)\right)\right)$$

$$\overline{\gamma} = 0.78\delta \pm 0.14\delta$$

Subsequent formulation: $\gamma(y) = \frac{1}{1+5.5\left(\frac{y}{\Delta}\right)^6}$

Where length scale $\Delta = f(\text{flow})$.

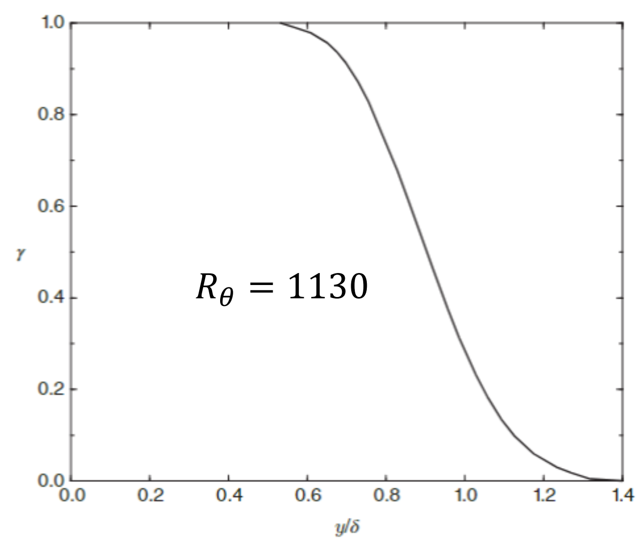

Figure 8.4 Intermittency factor in a turbulent boundary layer [5].

Boundary Layer Growth

Blasius laminar boundary layer:

$$\frac{\theta}{x} = \frac{0.664}{Re_x} \rightarrow \theta \propto \sqrt{x}$$

$$F_x = 0.664\frac{\rho U_\infty^2 L}{Re_L} \text{ per unit width}$$

Turbulent flow:

$$\frac{\partial \overline{U}^2}{\partial x} + \frac{\partial \overline{U}\,\overline{V}}{\partial y} = -\frac{1}{\rho}\frac{\partial \overline{p}}{\partial x} + \nu\frac{\partial^2 \overline{U}}{\partial y^2} - \frac{\partial \overline{uv}}{\partial y} \quad (1)$$

And

$$\frac{\partial}{\partial y}\left(\frac{\overline{p}}{\rho} + \overline{v^2}\right) = 0 \quad (2)$$

Since turbulence and viscous effects are confined in the BL, outer flow satisfies condition for Bernoulli's law:

$$\frac{U_0^2}{2} + \frac{p_0}{\rho} = \frac{U_\infty^2}{2} + \frac{\overline{p}}{\rho} \quad (3)$$

Constant on streamlines. Taking an x-derivative in Eq. (3) gives:

$$0 = \frac{\partial}{\partial x}\left(\frac{U_\infty^2}{2} + \frac{\overline{p}}{\rho}\right)$$

$$\frac{\partial \overline{p}}{\partial x} = -\rho U_\infty \frac{dU_\infty}{dx} \quad (4)$$

Similarly, taking an x-derivative of Eq. (2) yields:

$$\frac{\partial^2}{\partial x \partial y}\left(\frac{\overline{p}}{\rho} + \overline{v^2}\right) = 0 \rightarrow \frac{\partial}{\partial y}\left(\frac{\partial \overline{p}}{\partial x}\right) = 0$$

i.e., Eq. (4) applies across BL.

Substituting Eq. (4) into (1) and integrating normal to the wall to a point d where $\overline{U} = U_\infty$ gives:

$$\frac{\partial}{\partial x}\int_0^d \overline{U}^2 dy + U_\infty \overline{V}(x,d) = \int_0^d U_\infty \frac{dU_\infty}{dx} dy - \frac{\tau_w}{\rho} \quad (5)$$

$$\boxed{\overline{uv}|_0^d = 0}$$

Integrating the continuity equation across the boundary layer gives:

$$\int_0^d \frac{\partial \overline{V}}{\partial y} dy = -\int_0^d \frac{\partial \overline{U}}{\partial x} dy$$

$$\overline{V}(x,d) = -\int_0^d \frac{\partial \overline{U}}{\partial x} dy \quad (6)$$

And substituting Eq. (6) into (5) yields:

$$\frac{\partial}{\partial x}\int_0^d \overline{U}^2 dy - U_\infty \int_0^d \frac{\partial \overline{U}}{\partial x} dy = \int_0^d U_\infty \frac{dU_\infty}{dx} dy - \frac{\tau_w}{\rho}$$

$$\frac{d}{dx}\int_0^d \left(\overline{U}^2 - \overline{U} U_\infty\right) dy = \frac{dU_\infty}{dx}\int_0^d (U_\infty - \overline{U}) dy - \frac{\tau_w}{\rho}$$

$$\frac{d}{dx}\left[U_\infty^2 \int_0^d \frac{\overline{U}}{U_\infty}\left(\frac{\overline{U}}{U_\infty} - 1\right) dy\right] = \frac{dU_\infty}{dx} U_\infty \int_0^d \left(1 - \frac{\overline{U}}{U_\infty}\right) dy - \frac{\tau_w}{\rho} \quad (7)$$

Letting $d \to \infty$, since the integrands approach 0 as y increases to ∞, Eq. (7) becomes:

$$\frac{\tau_w}{\rho} = \frac{d}{dx}\left[U_\infty^2 \underbrace{\int_0^\infty \frac{\overline{U}}{U_\infty}\left(1 - \frac{\overline{U}}{U_\infty}\right) dy}_{\boxed{\theta(x)}}\right] + \frac{dU_\infty}{dx} U_\infty \underbrace{\int_0^\infty \left(1 - \frac{\overline{U}}{U_\infty}\right) dy}_{\boxed{\delta_1(x)}}$$

$$\frac{\tau_w}{\rho} = \frac{d}{dx}(U_\infty^2\,\theta) + \frac{dU_\infty}{dx} U_\infty \delta_1 \quad (8)$$

$$\frac{\tau_w}{\rho} = 2\theta U_\infty \frac{dU_\infty}{dx} + U_\infty^2 \frac{d\theta}{dx} + \frac{dU_\infty}{dx} U_\infty \delta_1$$

$$\frac{\tau_w}{\rho U_\infty^2} = \frac{2\theta}{U_\infty}\frac{dU_\infty}{dx} + \frac{d\theta}{dx} + \frac{dU_\infty}{dx}\frac{\delta_1}{U_\infty}$$

$$\frac{\tau_w}{\rho U_\infty^2} = \frac{d\theta}{dx} + (2 + H)\frac{\theta}{U_\infty}\frac{dU_\infty}{dx}$$

$$\boxed{H = \frac{\delta_1}{\theta} = \text{shape parameter}}$$

Representing the momentum integral equation for BL with pressure gradient. This equation represents $\tau_w = f(\delta_1, \theta)$.

Assuming a power law form of the mean velocity, similarly to what was done for pipe flow:

$$\overline{U} = U_\infty \left(\frac{y}{\delta}\right)^{1/n}$$

And substituting the power law $\overline{U}$ into the definitions of $\delta_1(x)$ and $\theta(x)$ yields:

$$\delta_1 = \frac{\delta}{1 + n}$$

$$\theta = \frac{\delta n}{(n+1)(n+2)}$$

Substituting these relations into Eq. (8) and taking $n = 7$ yields a dfferential equation for δ in the form:

$$\frac{7}{72}\frac{dU_\infty^2\theta}{dx} + \frac{1}{8}\frac{dU_\infty}{dx}U_\infty\delta = \frac{\tau_w}{\rho} \qquad (9)$$

Need for $\tau_w = f(\delta) \rightarrow$ power law fit data, for $U_\infty =$ constant:

$$\frac{\tau_w}{\rho} = 0.0225\frac{\nu^2}{\delta^2}Re_\delta^{7/4}$$

And substituting this into Eq. (9) gives:

$$\frac{d\delta}{dx} = 0.0225\frac{72}{7}\ Re_\delta^{-1/4}$$

i.e.,

$$\frac{\delta}{x} = 0.37Re_x^{-1/5}$$

$$\delta \propto x^{\frac{4}{5}} \gg x^{\frac{1}{2}}\ \text{laminar flow}$$

This result is consistent with EFD for $Re < 10^6$, for higher Re use $n = 8$ or higher.

π-β Method

As mentioned earlier, the momentum integral equation for turbulent flow has the identical form as the laminar-flow relation:

$$\frac{d\theta}{dx} = \frac{C_f}{2} - (2+H)\frac{\theta}{U_e}\frac{dU_e}{dx} \qquad \text{(I)}$$

With U(x) assumed known, there are three unknown C_f, H, θ for turbulent flow. Thus, at least two additional relations are needed to find unknowns. There are many possibilities for additional relations all of which require a certain amount of empirical data. As an example we will review the π−β method.

Cole's law of the wake:

By adding the wake to the log-law, the velocity profile for both overlap and outer layers can be written as:

$$u^+ = \frac{1}{\kappa}\ln y^+ + B + \frac{2\Pi}{\kappa} f(\eta)$$

where

$$\eta = y/\delta$$

$$f(\eta) = \sin^2\left(\frac{\pi}{2}\eta\right) = 3\eta^2 - 2\eta^3$$

$$\Pi = \kappa A/2$$

The quantity Π is called Coles' wake parameter.

By integrating wall-wake law across the boundary layer:

$$\lambda = a(\Pi)\frac{H}{H-1}$$

$$a(\Pi) = \frac{2 + 3.179\Pi + 1.5\Pi^2}{\kappa(1+\Pi)}$$

$$\text{Re}_\theta = \frac{U\theta}{\upsilon} = \frac{1+\Pi}{\kappa H}\exp(\kappa\lambda - \kappa B - 2\Pi)$$

If we eliminate Π between these formulas, we obtain a unique relation among $C_f = 2/\lambda^2$, H and θ:

$$\begin{cases} C_f = 2/\lambda^2 = 2/[a(\Pi)\dfrac{H}{H-1}]^2 \\ a(\Pi) = \dfrac{2+3.179\Pi+1.5\Pi^2}{\kappa(1+\Pi)} \\ \mathrm{Re}_\theta = \dfrac{U\theta}{\upsilon} = \dfrac{1+\Pi}{\kappa H}\exp(\kappa\lambda - \kappa B - 2\Pi) \end{cases} \qquad \text{(II)}$$

<u>Clauser's equilibrium parameter β:</u>

For outer layer,

$$U_e - \bar{u} = f(\tau_w, \rho, y, \delta, \frac{dp}{dx})$$

Using dimensional analysis:

$$\frac{U_e - \bar{u}}{(\tau_w/\rho)^{1/2}} = g(\frac{y}{\delta}, \frac{\delta}{\tau_w}\frac{dp}{dx})$$

Clauser (1954) replaced δ by displacement thickness δ^*:

$$\frac{U_e - \bar{u}}{(\tau_w/\rho)^{1/2}} = g(\frac{y}{\delta}, \beta)$$

$$\beta = \frac{\delta^*}{\tau_w}\frac{dp}{dx} = -\lambda^2 H \frac{\theta}{U_e}\frac{dU_e}{dx}$$

β is called Clauser's equilibrium parameter.

Das (1987) showed that EFD data points fit into the following polynomial correlation:

$$\beta = -0.4 + 0.76\Pi + 0.42\Pi^2$$

Therefore:

$$-\lambda^2 H \frac{\theta}{U_e}\frac{dU_e}{dx} = -0.4 + 0.76\Pi + 0.42\Pi^2 \qquad \text{(III)}$$

If we eliminate Π using that $Re_\theta = \frac{U\theta}{\upsilon} = \frac{1+\Pi}{\kappa H}\exp(\kappa\lambda - \kappa B - 2\Pi)$, we obtain another relation among $C_f = 2/\lambda^2$, H and θ.

Equations (I), (II), and (III) can be solved simultaneously using say a Runge-Kutta method to find C_f, H, θ. Equations are solved with initial condition for $\theta(x_0)$ and integrated to $x=x_0+\Delta x$ iteratively. Estimated θ gives Re_θ and Π, β gives H. Lastly C_f is evaluated using Re_θ and H. Iterations required until all relations satisfied and then proceed to next Δx.

Log-Law Behavior of the Velocity Mean and Variance

EFD up to $R_\tau = U_\tau \delta/\nu = 13600$.

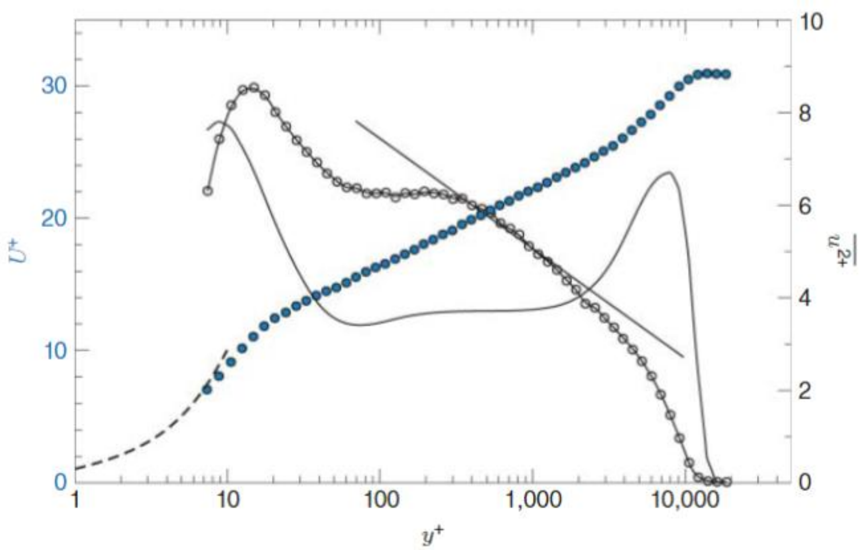

Figure 8.5 Mean and variance of the streamwise velocity in boundary layer flow at $R_\tau = 13{,}600$. •, $\overline{U}$; —, $y^+\partial\overline{U}^+/\partial y$; ○, $\overline{u^2}^+$; straight line is a fit to Eq. (8.25). Data from [11]. Figure reproduced from [12] by permission of Annual Reviews.

$$U^+ = \frac{1}{k}\log y^+ + B$$

$k = 0.41$, $B = 5.0$ for $30 \le y^+ \le 0.15\delta \rightarrow$ log law region.

Log-law indicator function:

$$y^+ \frac{\partial \overline{U}^+}{\partial y^+}$$

It is expected to be constant in the region where exact log-law behavior occurs, plot shows that for $y^+ < 100$ this function rises and then stays almost constant up to $y^+ = 2500$.

Similar behavior channel and pipe flow with primary differences due outer layer. Combining all these flows, log law found for $3\sqrt{R_\tau} \leq y^+ \leq 0.15 R_\tau$ with $k = 0.39$ and $B = 4.3$.

Attached eddy hypothesis Townsend:

$$\overline{u^2}^+ = B_1 - A_1 \log\left(\frac{y}{\delta}\right)$$

Where $A_1 = 2.39$ and $B_1 = 1.03$. This equation describes the measured normal stress in the outer part of log-law region, as per Fig. 8.5.

Townsend (1976), Page 153:

It is difficult to imagine how the presence of the wall could impose a dissipation length-scale proportional to distance from it unless the main eddies of the flow have diameters proportional to distance of their 'centres' from the wall because their motion is directly influenced by its presence. In other words, the velocity fields of the main eddies, regarded as persistent, organised flow patterns, extend to the wall and, in a sense, they are *attached* to the wall. We proceed to consider the observed characteristics of a motion made up from the superposition of attached eddies of a wide range of sizes.

Let us suppose that the main, energy-containing motion is made up of contributions from 'attached' eddies with similar velocity distributions,

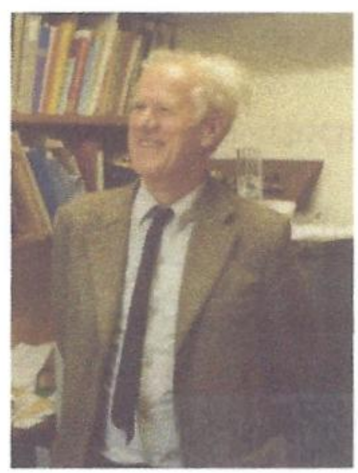

Outer Layer

Intermittency distinguishes BL outer region from channel and pipe flows, which reach fully developed condition vs BL spatially developing in streamwise direction. Also $\overline{V} \neq 0$, since $\overline{U_x} \neq 0$.

Outer flow scaling:

$$U_\infty - \overline{U}(y) = F\left(y, \delta, \rho, U_\tau, \frac{dP_\infty}{dx}\right) \neq f(\nu)$$

Using dimensional analysis:

$$\frac{U_\infty - \overline{U}(y)}{U_\tau} = U_\infty^+ - \overline{U}^+(y) = F\left(\frac{y}{\delta}, \underbrace{\frac{\delta}{\rho U_\tau^2}\frac{dP_\infty}{dx}}_{\text{equilibrium parameter}}\right) \quad (10)$$

If δ replaced by $\delta_1 =$ Clauser (1954, 1956) equilibrium parameter β.

EFD suggests that $U_\infty^+ - \overline{U}^+(y)$ for BL with different $\frac{dP_\infty}{dx}$ but same β collapses under same profile, so called turbulent equilibrium.

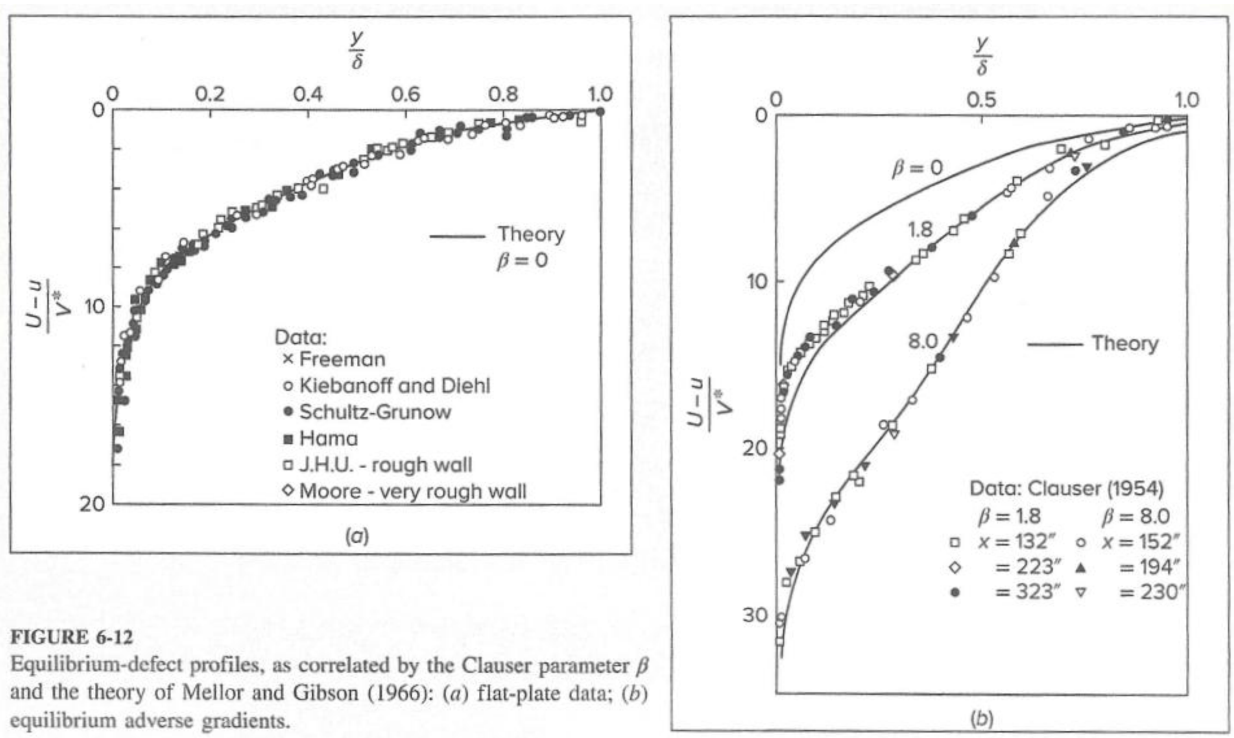

FIGURE 6-12
Equilibrium-defect profiles, as correlated by the Clauser parameter β and the theory of Mellor and Gibson (1966): (*a*) flat-plate data; (*b*) equilibrium adverse gradients.

The weakness of the Clauser approach to the outer layer is that the curves do not have a recognizable shape, which was resolved by Coles (1956) who notes the deviations of the velocity above the overlap layer when normalized by the maximum deviation at y = δ would be a single wake like function of y/δ only.

$\overline{U}(y)$ deviates from log-law for $0.15 \leq \frac{y}{\delta} \leq 1$.

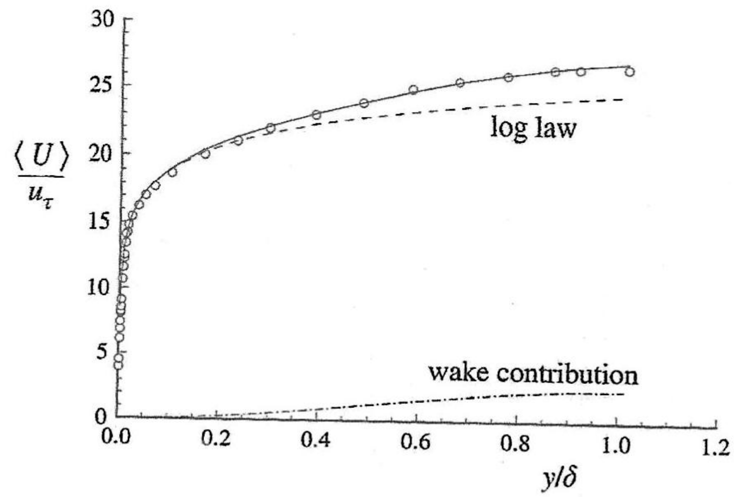

Fig. 7.28. The mean velocity profile in a turbulent boundary layer showing the law of the wake. Symbols, experimental data of Klebanoff (1954); dashed line, log law ($\kappa = 0.41, B = 5.2$); dot–dashed line, wake contribution $\Pi w(y/\delta)/\kappa$ ($\Pi = 0.5$); solid line, sum of log law and wake contribution (Eq. (7.148)).

Imposing Eq. (10) to match log-law in the intermediate layer gives (neglecting pressure gradient):

$$\frac{1}{k}\ln y^+ + B = U_\infty^+ - F\left(\frac{y}{\delta}\right)$$

So that $F\left(\frac{y}{\delta}\right)$ = difference between outer flow U_∞^+ and log-law.

For $y \ll \delta$, i.e., overlap region:

$$F\left(\frac{y}{\delta}\right) = U_\infty^+ - \left[\frac{1}{k}\ln y^+ + B\right] = \left[U_\infty^+ - \frac{1}{k}\ln \delta^+ - B\right] - \frac{1}{k}\ln\left(\frac{y}{\delta}\right)$$

$$\delta^+ = U_\tau\, \delta/\nu$$

For y/δ in both overlap, and outer regions include wake function $W\left(\frac{y}{\delta}\right)$.

$$F\left(\frac{y}{\delta}\right) = \left[U_\infty^+ - \frac{1}{k}\ln\delta^+ - B\right] - \frac{1}{k}\ln\left(\frac{y}{\delta}\right) - \frac{\Pi}{k}W\left(\frac{y}{\delta}\right) \quad (11)$$

$\frac{\Pi}{k}W\left(\frac{y}{\delta}\right)$ = amount that $\overline{U}^+$ rises above log-law in outer region beyond $y > 0.15\delta$, and is equal to 0 in log law region. Π is a parameter and $F + \frac{\Pi}{k}W$ is the difference between U_∞^+ and the log law extended into the outer layer.

Since, according to Eq. (10), $F\left(\frac{y}{\delta} = 1\right) = 0$:

$$W(1)\frac{\Pi}{k} = U_\infty^+ - \frac{1}{k}\ln\delta^+ - B \quad (12)$$

And combining this result with Eqs. (10) and (11) gives the Coles "law of the wake":

$$\overline{U}^+ = \frac{1}{k}\ln y^+ + B + \frac{\Pi}{k}W\left(\frac{y}{\delta}\right)$$

$$= \frac{1}{k}\ln y^+ + B + \frac{W\left(\frac{y}{\delta}\right)}{W(1)}\left(U_\infty^+ - \frac{1}{k}\ln\delta^+ - B\right)$$

i.e.,

$$\frac{W\left(\frac{y}{\delta}\right)}{W(1)} = \frac{\overline{U}^+ - \frac{1}{k}\ln y^+ - B}{U_\infty^+ - \frac{1}{k}\ln\delta^+ - B}$$

Representing the fractional velocity deficit relative to the log-law.

Empirical models:

$$\frac{\Pi}{k} W\left(\frac{y}{\delta}\right) = 2\frac{\Pi}{k}\sin^2\left(\frac{\pi}{2}\frac{y}{\delta}\right)$$

or

$$\frac{\Pi}{k} W\left(\frac{y}{\delta}\right) = \frac{1}{k}(1+6\Pi)\left(\frac{y}{\delta}\right)^2 - \frac{1}{k}(1+4\Pi)\left(\frac{y}{\delta}\right)^3$$

Where the latter is more accurate and $W(1) = 2$ is enforced in both models.

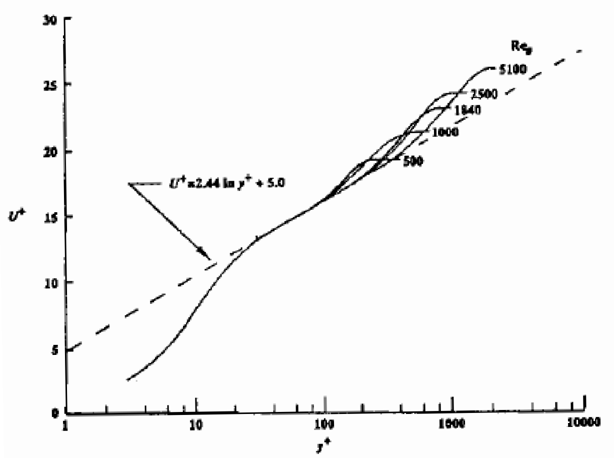

Fig 10. Comparison of mean-velocity profiles with logarithmic law at low Reynolds numbers. Boundary layer data from Purtell *et al* (1981).

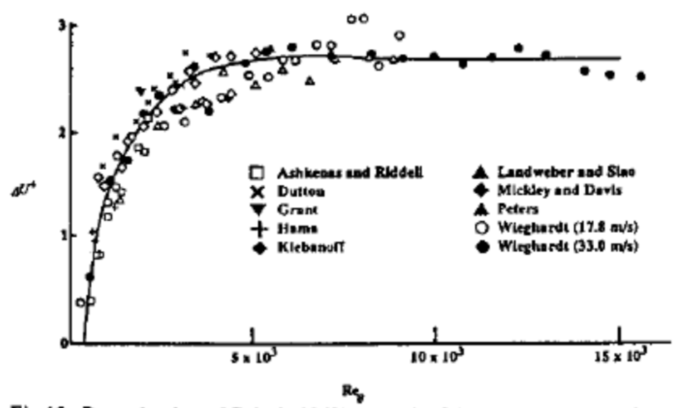

Fig 13. Reproduction of Coles' (1962) strength of the wake component in equilibrium turbulent boundary layers at low Reynolds numbers.

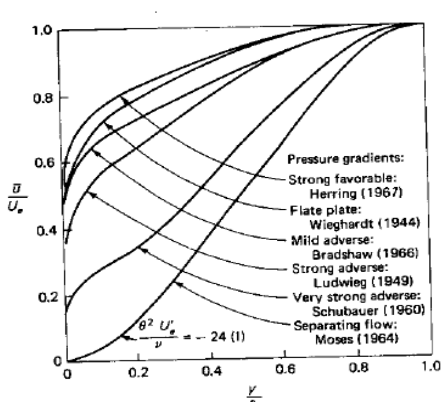

FIGURE 6-8
Experimental turbulent-boundary-layer velocity profiles for various pressure gradients. [*Data from Coles and Hirst (1968).*]

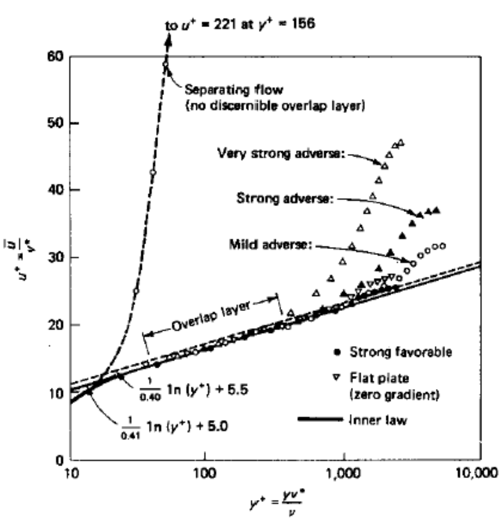

FIGURE 6-9
Replot of the velocity profiles of Fig. 6-8 using inner-law variables y^+ and u^+.

According to Eq. (12),

$$\Pi = f(U_\infty^+, \delta^+) = f(x)$$

For zero-pressure gradient, it follows from

$$\frac{\delta}{x} = 0.37 Re_x^{-1/5}$$

That

$$Re_\delta = \frac{\delta U_\infty}{\nu} = 0.37 Re_x^{4/5}$$

$$\delta = 0.37 x Re_x^{-1/5}$$

$$\frac{U_\infty \delta}{\nu} = 0.37 \frac{U_\infty x}{\nu} Re_x^{-1/5}$$

Where $Re_x = xU_\infty/\nu$.

Using

$$U_\tau^2 = \frac{\tau_w}{\rho} = 0.0225 \frac{\nu^2}{\delta^2} Re_\delta^{7/4}$$

Gives

$$U_\infty^+ = \frac{U_\infty}{U_\tau} = 5.89 Re_x^{1/10}$$

$$\delta^+ = 0.0628 Re_x^{7/10}$$

Recall Eq. (12):

$$W(1)\frac{\Pi}{k} = U_\infty^+ - \frac{1}{k}\ln \delta^+ - B$$

$$\Pi = \frac{k}{2}\left(5.89 Re_x^{\frac{1}{10}} - \frac{1}{k}(-2.77 + 0.7\ln(Re_x)) - B\right)$$

Which is slowly varying with x, e.g., with $k = 0.4$, $B = 5.1$ and Re_x ranging from 5×10^6 to 10^7, Π varies from 0.48 to 0.63. Typically, $\Pi = 0.55$ is used.

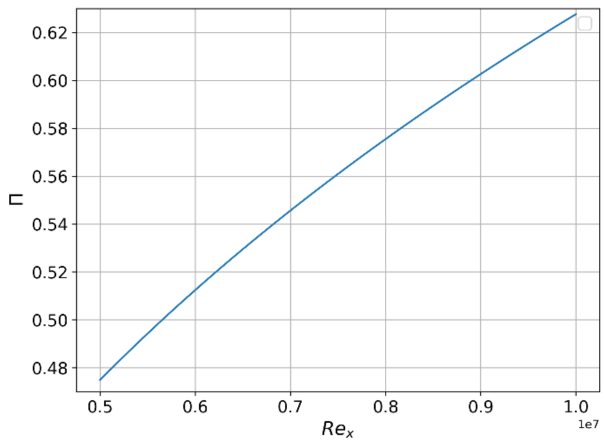

Variation of Π vs Re_x.

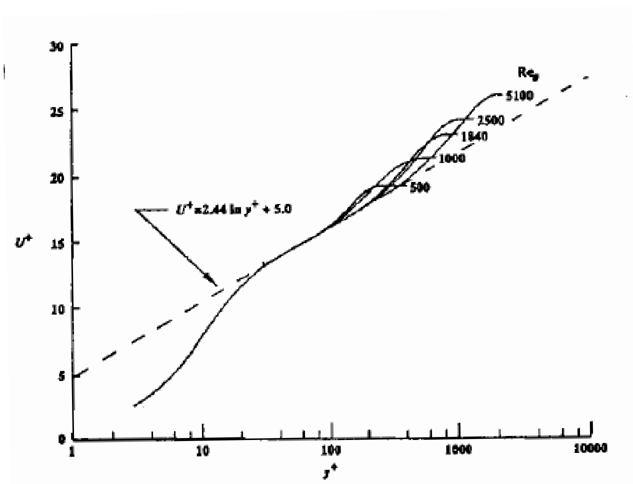

Fig 10. Comparison of mean-velocity profiles with logarithmic law at low Reynolds numbers. Boundary layer data from Purtell *et al* (1981).

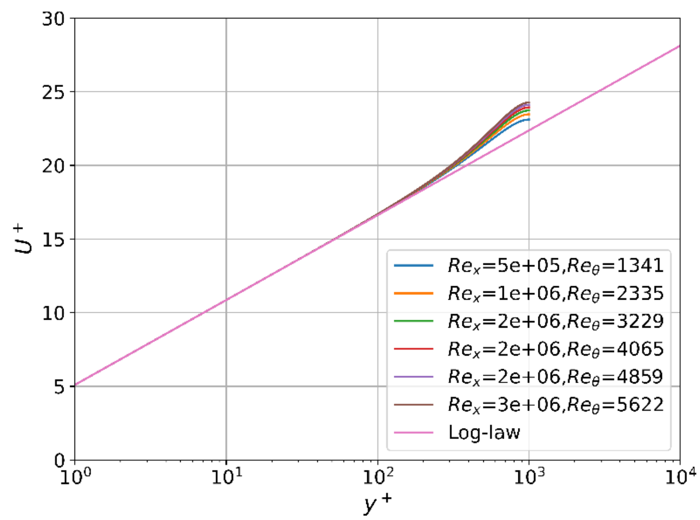

Re_x	$Re_\theta = 0.037Re_x^{4/5}$
5×10^5	8460
1×10^6	2334
1.5×10^6	3229
2×10^6	4605
2.5×10^6	4859
3×10^6	5622

Comparison of mean velocity profile with logarithmic law using:

$$\overline{U}^+ = \frac{1}{k}\ln y^+ + B + \frac{\Pi}{k} W\left(\frac{y}{\delta}\right)$$

$$\Pi = \frac{k}{2}\left(5.89Re_x^{\frac{1}{10}} - \frac{1}{k}(-2.77 + 0.7\ln(Re_x)) - B\right)$$

$$k = 0.4, \quad B = 5.1$$

Alternative Π = wake parameter = $\Pi(\beta)$ including pressure gradient:

$$\Pi(\beta) = 0.8(\beta + 0.5)^{0.75} \rightarrow \text{(curve fit for data)}$$

Note that for $\beta = 0$ $\Pi = 0.48$ and the agreement of Coles' wake law even for $\beta \neq$ constant. Bl's is quite good.

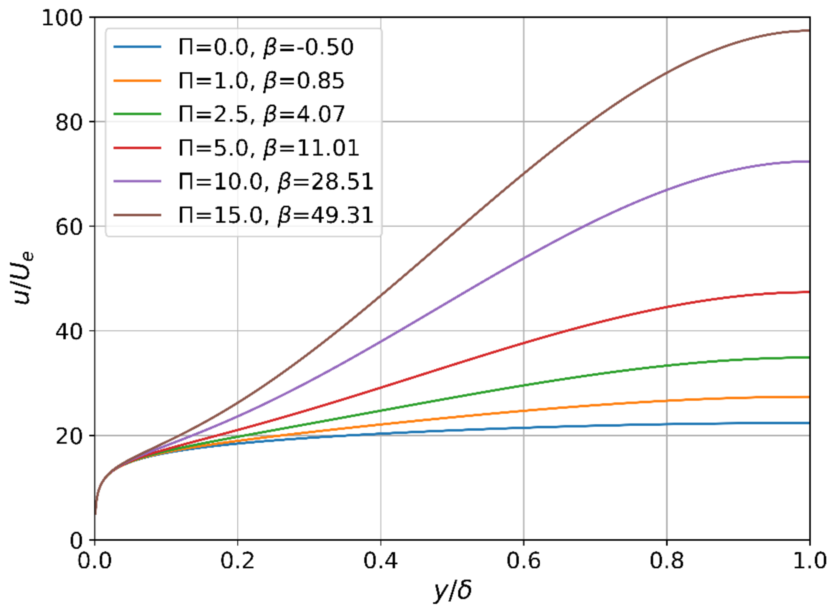

Turbulent velocity profiles computed from the Coles wall-wake formula

$$\overline{U}^{+} = \frac{1}{k}\ln y^{+} + B + \frac{\Pi}{k} W\left(\frac{y}{\delta}\right)$$

Assuming $\delta^{+} = 1000$. The curve for $\Pi = 0$ is the pure law of the wall. Note that the plot starts at $y^{+} = 1$ or $y/\delta = 0.001$.

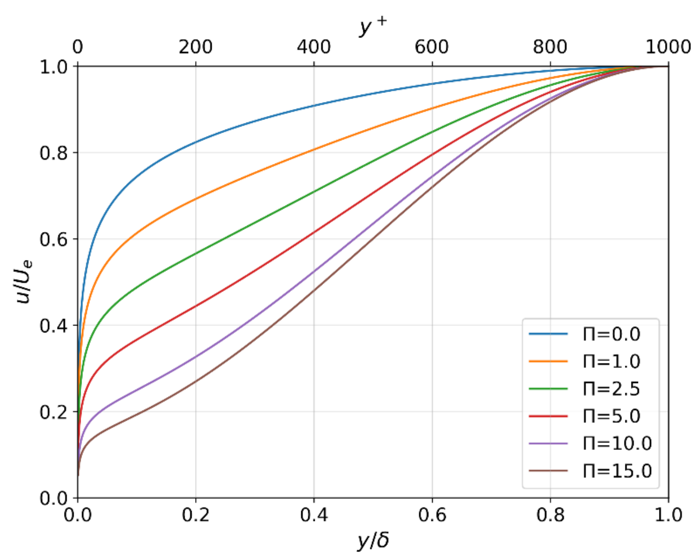

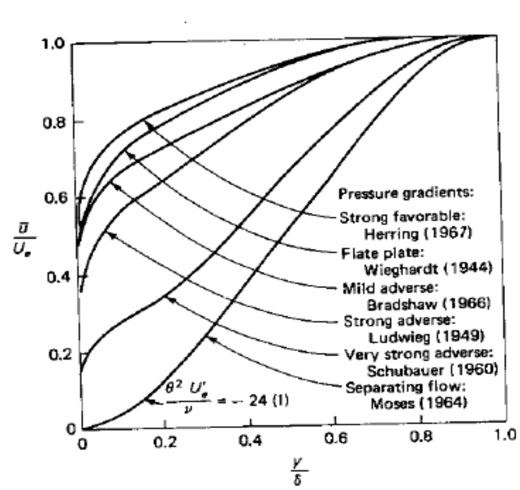

Recent research:

Zero-pressure-gradient turbulent boundary layer

William K George and Luciano Castillo

State University of New York at Buffalo, Buffalo NY 14260; trlbill@eng.buffalo.edu

Of the many aspects of the long-studied field of turbulence, the zero-pressure-gradient boundary layer is probably the most investigated, and perhaps also the most reviewed. Turbulence is a fluid-dynamical phenomenon for which the dynamical equations are generally believed to be the Navier-Stokes equations, at least for a single-phase, Newtonian fluid. Despite this fact, these governing equations have been used in only the most cursory manner in the development of theories for the boundary layer, or in the validation of experimental data-bases. This article uses the Reynolds-averaged Navier-Stokes equations as the primary tool for evaluating theories and experiments for the zero-pressure-gradient turbulent boundary layer. Both classical and new theoretical ideas are reviewed, and most are found wanting. The experimental data as well is shown to have been contaminated by too much effort to confirm the classical theory and too little regard for the governing equations. Theoretical concepts and experiments are identified, however, which are consistent–both with each other and with the governing equations. This article has 77 references.

AIAA JOURNAL
Vol. 39, No. 1, January 2001

Similarity Analysis for Turbulent Boundary Layer with Pressure Gradient: Outer Flow

Luciano Castillo*
Rensselaer Polytechnic Institute, Troy, New York 12180
and
William K. George†
State University of New York at Buffalo, Buffalo, New York 14260

The equilibrium-type similarity analysis of George and Castillo for the outer part of zero pressure gradient boundary layers (George, W. K., and Castillo, L., "Zero Pressure Gradient Turbulent Boundary Layer," *Applied Mechanics Reviews*, Pt. 1, Vol. 50, No. 11, 1997, pp. 689–729) has been extended to include boundary layers with pressure gradient. The constancy of a single new pressure gradient parameter is all that is necessary to characterize these new equilibrium turbulent boundary layers. Three major results are obtained: First, most pressure gradient boundary experiments appear to be equilibrium flows (by the new definition), and nonequilibrium flows appear to be the exception. Second, there appear to be only three values of the pressure gradient parameter: one for adverse pressure gradients, one for favorable pressure gradients, and one for zero pressure gradients. Third, correspondingly, there appear to be only three normalized velocity deficit profiles, exactly as suggested by the theory.